論文 / 著書情報
Article / Book Information

Title	Sidelobe suppression in both the E and H planes using slit layers over a corporate-feed waveguide slot array antenna consisting of 2×2-element radiating units
Authors	Haruka Arakawa, Takashi Tomura, Jiro Hirokawa
Citation	IEICE TRANSACTIONS on Communications, vol. E103-B, no. 9, pp. 960-968
Pub. date	2020, 9
Copyright	Copyright (c) 2020 Institute of Electronics, Information and Communication Engineers.

IEICE TRANS. COMMUN., VOL.E103–B, NO.9 SEPTEMBER 2020

PAPER

Sidelobe Suppression in Both the E and H Planes Using Slit Layers over a Corporate-Feed Waveguide Slot Array Antenna Consisting of 2×2-Element Radiating Units

Haruka ARAKAWA[†a)], **Takashi TOMURA**[†], ***Members***, ***and*** **Jiro HIROKAWA**[†], ***Fellow***

SUMMARY The sidelobe level at tilts around 30–40 degrees in both the E and H planes due to a tapered excitation of units of 2×2 radiation slots is suppressed by introducing slit layers over a corporate-feed waveguide slot array antenna. The slit layers act as averaging the excitation of the adjacent radiating slots for sidelobe suppression in both planes. A 16×16-element array in the 70 GHz band is fabricated. At the design frequency, the sidelobe levels at tilts around 30–40 degrees are suppressed from −25.4 dB to −31.3 dB in the E-plane and from −27.1 dB to −38.9 dB in the H-plane simultaneously as confirmed by measurements. They are suppressed over the desired range of 71.0–76.0 GHz frequencies, compared to the conventional antenna.

key words: *full-corporate-feed, millimeter-wave antenna arrays, Taylor distribution, waveguide slot arrays*

1. Introduction

A low sidelobe antenna is becoming a very important component to realize high-speed point-to-point fixed wireless access in backhaul system using a millimeter wave because of the growing demand for higher data-rate transmission. According to the European Telecommunications Standards Institute (ETSI), there are four classes of standard radiation pattern envelopes (RPEs) depending on the interference risk in the network [1] and many researches have been reported applied to the RPEs [2], [3]. To realize the low sidelobe antennas, a Taylor distribution is applied to aperture antennas [4]–[8], that is a well-known amplitude-taper method for sidelobe suppression. However, radiation and dielectric losses in a microstrip aperture array antenna are indispensable with higher frequency, a waveguide slot array antenna is more suitable for the millimeter wave due to low transmission loss. One possible application of a low sidelobe waveguide slot array antenna applied to a Taylor distribution is a directional division duplex (DDD) system which is capable of simultaneous bi-directional communication with same frequency and same polarization [9]. This system doubles the frequency utilization efficiency of the traditional duplex systems and requires a low sidelobe antenna to minimize interferes between the Tx and Rx antennas. The authors proposed a double-layer plate-laminated waveguide slot array antenna, which applies a Taylor distribution [10] by a series-feed circuit [11], [12]. The proposed antenna has achieved desired characteristics over 39.5–41.0 GHz [12].

To broaden the range of the operating frequency, Watarai et al. applied to a full-corporate waveguide slot array antenna [13], which has a wider bandwidth characteristic of high gain and high efficiency in the 60 GHz-band [14]. That antenna has double layers. The corporate-feed circuit is placed on the bottom layer. It consists of H-plane T-junctions, which divide a power equally at any frequencies. Each end of the feeding waveguide has a resonant coupling slot. It excites 2×2 radiating slots almost equally both in amplitude and in phase as a unit through a cavity on the top layer. This antenna can be built up by diffusion bonding of laminated thin copper etched plates [15] as a commercially available fabrication technique with advantageous features of high accuracy, reproducibility, and reliability.

When a Taylor distribution is applied to the full-corporate-feed waveguide slot array antenna in the E and H planes, the amplitude taper is realized by controlling a power providing to each coupling slot by the cascaded T-junctions which are asymmetrical but do not have any large phase differences in the corporate-feed circuit at the design frequency [14]. However, 2×2 radiating slots in each unit are equally excited and the unit spacing is around 1.66 λ_0 where λ_0 is the wavelength in free space at the design frequency, the sidelobe level at tilts around 30–40 degrees increases to −22.6 dB. Similar behaviors were reported in a prototype fabricated by a milling technique with aluminum in the Ku-band [16].

To suppress the high sidelobes, Qin et al. introduced a narrow trench, which is cut from the underside of exciting slots facing the cavity along the H-plane and divides power to a pair of radiating slots unequally in the E-plane in each radiating unit in 32×64-element array in 70 GHz-band [17]. As a result, this unequal power division helps to smooth the amplitude distribution at the radiating slots in the E-plane and suppresses the high sidelobes. However, the divided power ratios are controlled by the offset of the trench from the center along the E-plane and are different among the subarrays. This structure needs to be designed for each subarray individually and this method isn't effective for the H-plane.

Whereas, we introduced a double slit layer over a

Manuscript received September 27, 2019.
Manuscript revised January 5, 2020.
Manuscript publicized March 16, 2020.

[†]The authors are with the Department of Electrical and Electric Engineering, Tokyo Institute of Technology, Tokyo, 152-8552 Japan.
a) E-mail: arakawa.h@antenna.ee.titech.ac.jp

DOI: 10.1587/transcom.2019EBP3204

16×16-element array to suppress the high sidelobes at tilts 30–40 degrees in the E-plane [18]. Each slit layer has 17 lines along the H-plane and the slit spacing is the same with a slot spacing d and the radiating slots and slits are shifted by $d/2$ in the E-plane, so that this structure needs to be designed for one subarray. The double slit layer act as averaging the excitation of the adjacent radiating slots in the E-plane and suppress the high sidelobes. In this case, the aperture field at the radiating slots has a Taylor distribution in the E-plane and a uniform distribution in the H-plane as a unit of 2×2-radiating slots.

In this paper, we propose antennas suppressing the high sidelobes at tilts 30–40 degrees in the H-plane and in both the E and H planes based on [18]. In the H-plane, we have introduced a slit layer over a 16×16-element array where aperture distribution is a Taylor distribution in the H-plane and a uniform distribution in the E-plane as a unit of 2×2-radiating slots. The slit layer has 17 lines along the E-plane, averages the excitation of the adjacent radiating slots in the H-plane and suppresses the high sidelobes. Based on the result of the sidelobe suppression in the E and H-planes, we have designed the sidelobe suppression antenna in both the E and H planes. The design frequency is 73.5 GHz and a desired range of frequencies is 71.0–76.0 GHz.

This paper is organized as follows. Section 2 describes the antenna configuration and the operation. In Sect. 3, we propose the sidelobe suppressing antenna in the H-plane and compare the designed parameters and the operation between the E-plane and the H-plane sidelobe suppressing antennas. In Sect. 4, we design the sidelobe suppressing antenna in both the E and H planes based on the combination of those in the E and H-planes and show the results of the analysis of the full structure. Section 5 describes the measured results with a prototype. Finally, the conclusion is detailed in Sect. 6.

2. Antenna Configuration and Operation

Figure 1(a) shows the configuration of the proposed sidelobe suppressing antenna in the E and H planes. The electric field and the magnetic field are oriented in the x and y-directions, respectively. To suppress the E and H-plane sidelobes at tilts around 30–40 degrees, we introduce slit layers over a 16×16-element array antenna. The slit layers have two parts. One part is for the E-plane sidelobe suppression and the other one is for the H-plane sidelobe suppression. The part for the E-plane sidelobe suppression consists of an E-plane slit layer of 17 lines with a PTFE substrate where relative permittivity is 2.18 and an air layer 1. The part for the H-plane consists of a H-plane slit layer of 17 lines and an air layer 2. The radiating slots array has a constant element spacing d (3.40 mm: $0.83\,\lambda_0$, where λ_0 is the wavelength in free space at the design frequency) in the x and the y-directions. The E and H-plane slits are arrayed at intervals of d and are shifted against the radiating slot by $d/2$ in the x and the y-directions, respectively.

The waveguide slot array antenna consists of a corporate-feed circuit in the feeding part, as shown in Fig. 1(b), and a 16×16-element slot array composed of a 2×2-element subarray in the radiating part, as shown in Fig. 1(c). The feeding circuit consists of the H-plane T-junctions and is fed by a feeding aperture of the standard rectangular waveguide WR-12 size from the back. Each end of the feeding circuit has a resonant coupling slot. It excites the 2×2 radiating slots equally both in amplitude and in phase as a unit so that radiating unit is $1.66\,\lambda_0$ ($2d$) in each plane, so that the grating lobes come out at tilts around 30–40 degrees in both planes when a Taylor distribution is applied to the waveguide slot array antenna in the both planes [14]. To suppress the

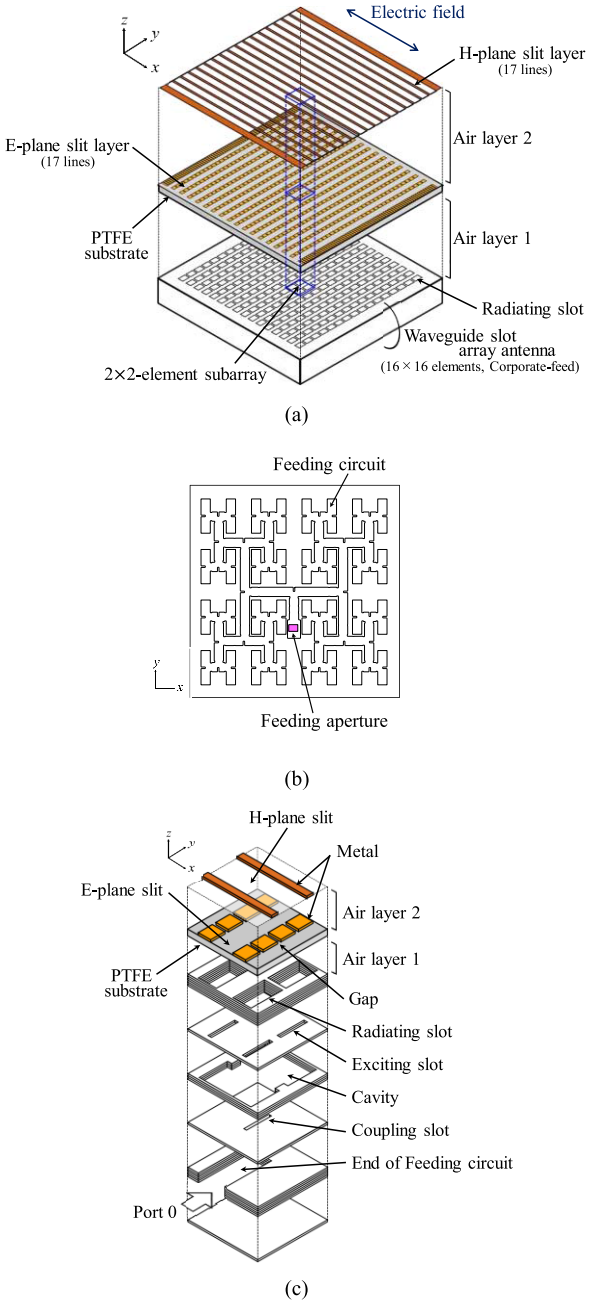

Fig. 1 Sidelobe suppressing antenna in both the E and H planes. (a) Full structure. (b) Corporate-feed circuit. (c) 2×2-element subarray.

high sidelobes, the proposed double slit layer act as averaging the excitation of the adjacent radiating slots in each plane, so that the radiating unit becomes 0.83 λ_0 (d) and the grating lobes at tilts around 30–40 degrees in the both planes are suppressed. Furthermore, to improve a degradation of a directivity around the design frequency due to a higher mode generating under the E-plane slit layer as discussed later, we introduce gaps in the metal part of the E-plane slit layer and cut off the surface current in the y-direction caused by the higher mode.

3. Sidelobe Suppression Antenna in Only the H-Plane

We proposed a sidelobe suppressing antenna in the E-plane (called as E-plane antenna thereafter) [18], as shown in Fig. 2. To average the excitation of the adjacent radiating slots in the E-plane, we introduce a slit layer 1 of 17 lines with a PTFE substrate and an air layer 1. We designed the antenna using 2×2-element subarray including the periodicity in the E- and H-planes and 8(E)×2(H) elements, that is a E-plane array, including the symmetry with respect to the E-plane and the periodicity in the H-plane. The three designed parameters which are the width of the slit 1, the thickness of the PTFE substrate and that of the air layer 1 are shown in Table 1 and the frequency characteristics of the sidelobe level at tilts around 30–40 degrees are shown in Fig. 4. The sidelobe level of the E-plane antenna is suppressed over 70.0–76.5 GHz when compared to a conventional E-plane antenna without the double slit layer in the simulation.

Before we design the sidelobe suppressing antenna in both the E and H planes, we present the design and the results of a sidelobe suppressing antenna in only the H-plane (called as H-plane antenna thereafter), as shown in Fig. 3. To average the excitation of the adjacent radiating slots in the H-plane, we introduce a slit layer 1 of 17 lines with a PTFE substrate and an air layer 1. In the same way as the E-plane antenna, we design the antenna using 2×2-elemnt subarray and 2(E)×8(H)-element array, that is a H-plane array, including the symmetry with respect to the H-plane and the periodicity in the E-plane, as shown in Fig. 3. The three designed parameters are shown in Table 1 and the frequency characteristics of the sidelobe level at tilts around 30–40 degrees are shown in Fig. 4. The sidelobe level of the H-plane antenna is suppressed over 71.0–78.0 GHz when compared to a conventional H-plane antenna without the slit layer 1 in the simulation.

Comparing the designed parameters between the E-plane and H-plane antennas, there are three differences in the operating principles depending on the direction of the electric field against the sidelobe suppressing plane. One is the difference in the width of the slit 1, which comes from the difference in the directions of the electric field and the slit 1. The electric field is parallel to the slit 1 in the H-plane antenna, while the electric field is perpendicular to the slit 1 in the E-plane antenna. For the electric field to pass through the slit 1, the width of the slit 1 in the H-plane antenna is needed to be wider than that in the E-plane antenna.

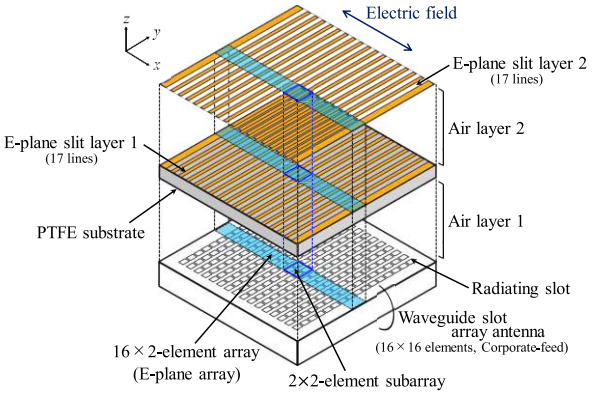

Fig. 2 Sidelobe suppressing antenna in the E-plane.

Table 1 Value of the parameters.

	E-plane antenna	H-plane antenna
Width of the slit 1	2.20 mm	3.00 mm
Thickness of the PTFE substrate	0.56 mm	0.19 mm
Thickness of the air layer 1	0.40 mm	2.00 mm
Electrical sum length of the thickness of the PTFE substrate and the air layer 1	0.30 λ_0	0.55 λ_0
Equivalent wavelength of the PTFE substrate and the air layer 1	3.33 mm	3.98 mm

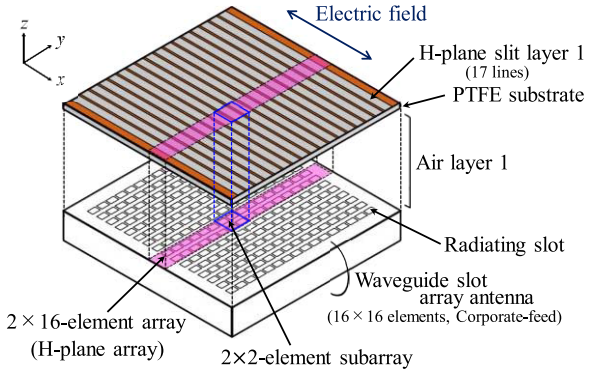

Fig. 3 Sidelobe suppressing antenna in the H-plane.

The second is the difference in the electrical sum length of the thickness of the PTFE substrate and the air layer 1, which is caused by the difference in the reflection suppressing mechanism. The top interface of the PTFE substrate is dominated by metal in the E-plane antenna so that the effective reflection coefficient there becomes negative (consider the reflection coefficient for a metal is −1), while that is dominated by gap in the H-plane antenna so that the effective reflection coefficient there becomes positive (consider the reflection coefficient from dielectric to air is positive). Therefore the electrical sum length of the thickness of the PTFE substrate and the air layer 1 is about $\lambda_0/4$ in the E-plane antenna while that in the H-plane antenna is about $\lambda_0/2$, con-

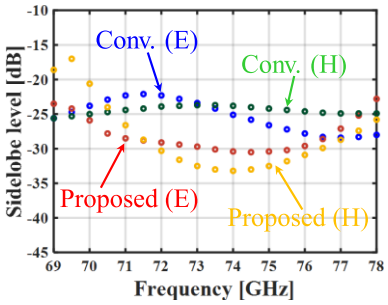

Fig. 4 Frequency characteristics of the sidelobe level at tilts around 30–40 degrees.

sidering the reflection coefficient at the top interface of the radiating slots is negative.

The last is the difference in the thickness ratio of the PTFE substrate and the air layer 1, which affects the excitation of the adjacent radiating slots. In the E-plane antenna, the equivalent wavelength in the x-direction in the region of the PTFE substrate and the air layer 1 is close to the spacing of the radiating slots so that a standing wave is excited in the region. In the H-plane antenna, the equivalent wavelength in the y-direction in the region of the PTFE substrate and the air layer 1 is close to the free-space wavelength so that such behavior does not occur.

4. Design

4.1 Sidelobe Suppressing Antenna in Both the E and H Planes

Based on the sidelobe suppressing antennas in the E-plane and H-plane, we propose the sidelobe suppressing antenna in both the E and H planes as shown in Fig. 5. To suppress the reflection, we place a E-plane slit layer and a H-plane slit layer with the spacing of about $0.30\,\lambda_0$ and $0.67\,\lambda_0$ in electrical length from the radiating slots, which are almost unchanged from the design values of the E-plane slit layer and the H-plane slit layer shown in Table 1. This means the mutual effect between the two slit layers is small. In Table 1, the thickness of the PTFE thickness for the H-plane antenna is 0.19 mm, which is much smaller than that for the E-plane antenna of 0.56 mm. After combing the E-plane slit layer and the H-plane slit layer, a dielectric substrate is still required for the E-plane layer to control the wavelength, however a dielectric can be omitted by adjusting the slit dimensions. To average the excitation of the adjacent radiating slots in the E-plane, the PTFE substrate and the air layer 1 are set under the E-plane slit layer and the equivalent wavelength in the PTFE substrate and the air layer 1 is about 3.4 mm, which is the wavelength in a parallel plate having the PTFE of 0.56 mm thickness and the air layer of 0.40 mm thickness. We design the antenna using 2×2-element subarray including the periodicity in the E- and H-planes and 8(E)×8(H) elements including the symmetry with respect to the E- and H-planes, as shown in Fig. 5(b) and (c). The values of the designed parameters are shown in Table 2 and the frequency

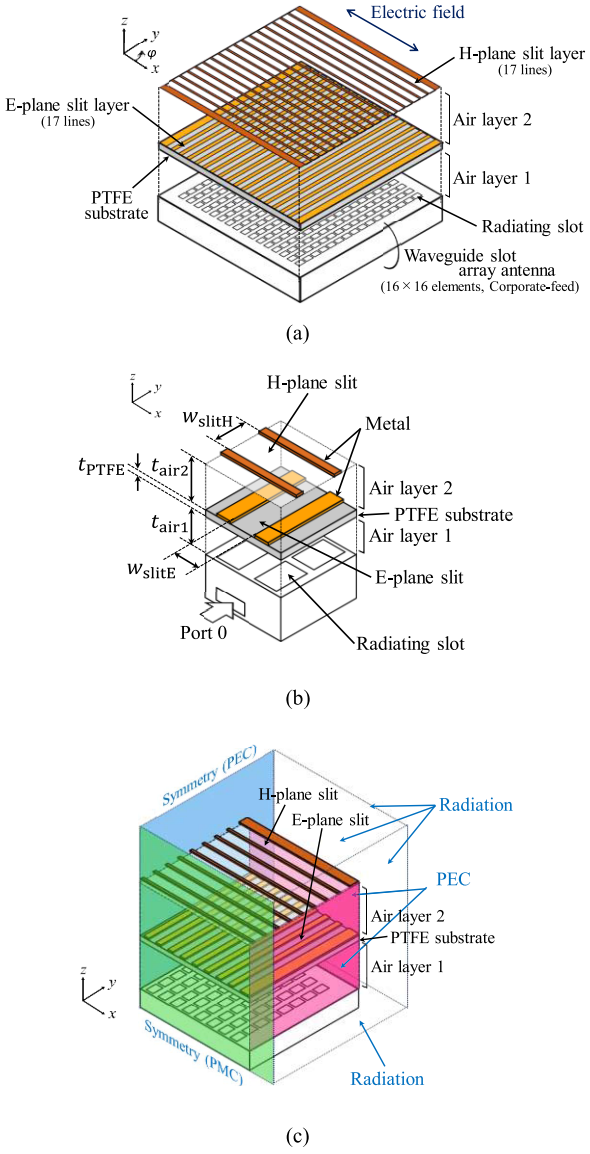

Fig. 5 Proposed antenna suppressing sidelobes in both the E and H planes. (a) Full structure. (b) 2×2-element subarray. (c) 8×8-element array.

Table 2 Value of the parameters.

Width of the H-plane slit	2.80 mm
Thickness of the air layer 2	1.50 mm
Width of the E-plane slit	2.20 mm
Thickness of the PTFE substrate	0.56 mm
Thickness of the air layer 1	0.40 mm
Electrical length of the distance from the radiating slot to the E-plane slit	0.30 λ_0
Electrical length of the distance from the radiating slot to the H-plane slit	0.67 λ_0

characteristic of the reflection and directivity in the 8×8 elements is shown in Fig. 6(a) and (b), respectively. The frequency characteristic of the reflection is achieved to VSWR

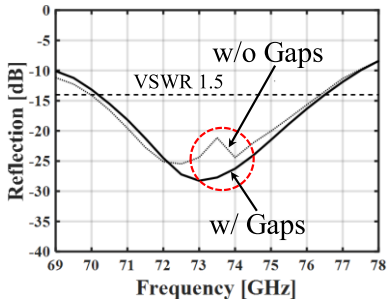

(a)

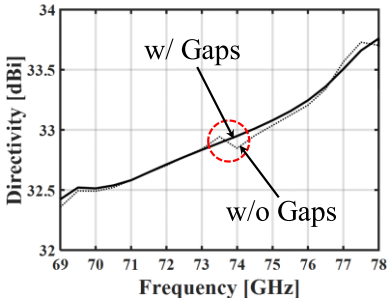

(b)

Fig. 6 Frequency characteristics in proposed antenna with and without gaps. (a) Reflection. (b) Directivity of the main polarization.

< 1.5 over the desired range of 71.0–76.0 GHz frequencies, but this has a ripple around 74 GHz as shown in Fig. 6(a). The frequency characteristic of the directivity has degraded locally around 74 GHz as shown in Fig. 6(b). Figure 7(a) shows the surface current at 74 GHz on the E-plane slit layer in the 8×8-element array in the actual simulation model and Fig. 7(b) is the drawing of the model, that is easier to understand the direction of the surface current than the actual simulation model. We find this degradation around 74 GHz is caused by the electric field oriented in the y-direction and makes the surface current on the E-plane slit layer flow in the y-direction as the cross polarization as shown in Fig. 7.

4.2 Improvement of the E-Plane Slit Layer

To suppress the undesired currents, we introduce gaps in the metal part of the E-plane slit layer. The length of the gaps is 0.2 mm along with the y-direction and the gap spacing is $d/2$ at the slits arranging periodically and $d/4$ at the right-side edge to suppress the undesired currents as shown in Fig. 8. At the right-side edge, the gap spacing of $d/2$ is not enough to suppress them. As a result, the degradation of the directivity around 74 GHz is removed and the directivity increases monotonously with frequency, as shown in Fig. 6(b).

4.3 Simulation of the Full Structure

The full structure of the proposed antenna is simulated by assuming a conductivity of 5.8×10^7 S/m of copper and a loss tangent of 0.0006 of PTFE. The post-walls are introduced at the side of the PTFE layer in place of the PEC.

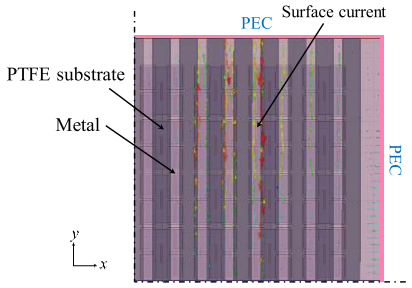

(a)

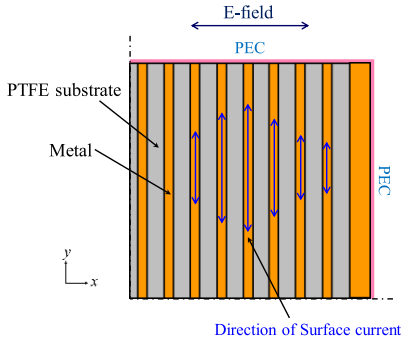

(b)

Fig. 7 Surface current on the E-plane suppression slit in the 8×8-element array. (a) The image of the actual simulation model. (b) The drawing of the model.

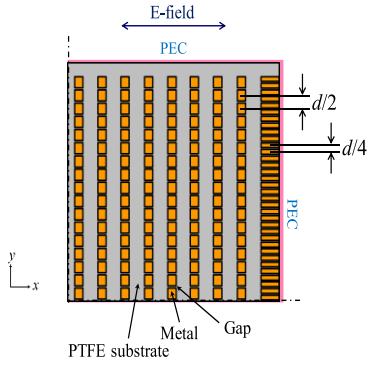

Fig. 8 Redesign of E-plane slit layer in the 8×8-element array.

Figure 9 shows the frequency characteristics of the reflections, together with those of the 2×2-element subarray and the corporate-feed circuit. The reflection of the full structure has ripples caused by the corporate-feed circuit. The bandwidth for VSWR < 1.5 is 9.0% (69.8–76.4 GHz).

Figure 10 shows the frequency characteristics of the directivity and the realized gain. The efficiency is estimated for the proposed antenna aperture size of 57.8 mm (= 3.4 mm×17 mm) square. At the design frequency, the calculated results are 32.8 dBi directivity, 76.2% aperture efficiency, 32.5 dBi realized gain, and with a 71.1% antenna efficiency.

Figure 11 shows the radiation patterns at the design frequency. Figure 11(a) and (b) show the radiation patterns of the main polarization in the E and H-plans. The sidelobe

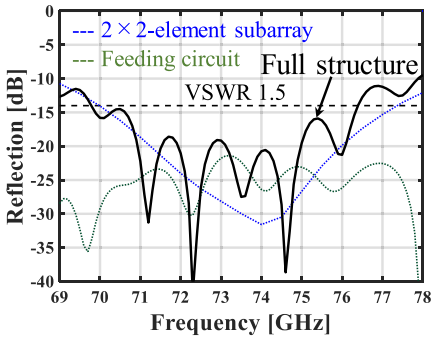

Fig. 9 Frequency characteristic of reflections in the simulation.

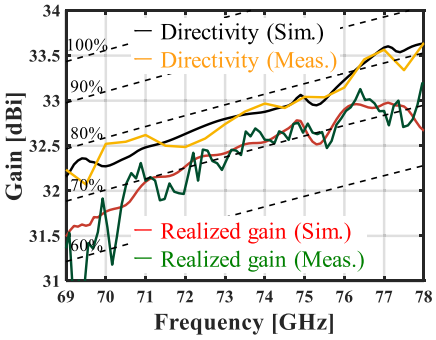

Fig. 10 Frequency characteristics of the directivity and realized gain.

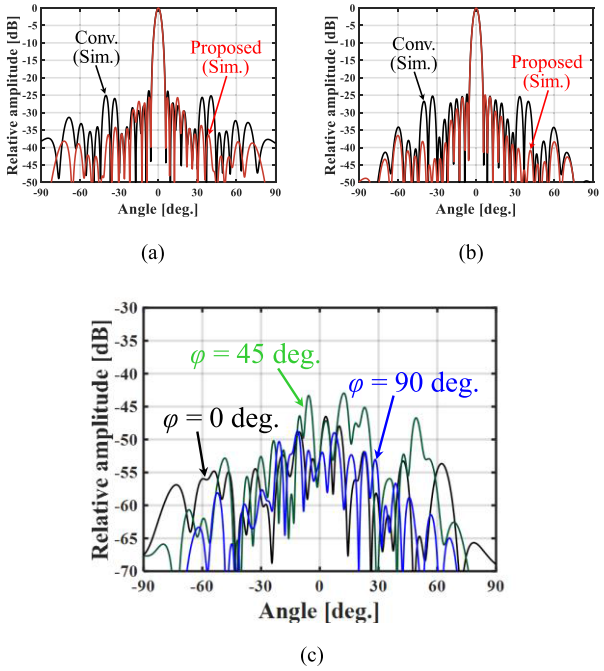

Fig. 11 Radiation patterns at the design frequency in the simulation. (a) E-plane. (b) H-plane. (c) Cross polarization (ϕ: 0, 45, 90 deg.).

level at tilts around 30–40 degrees is suppressed to −33.7 dB from −25.5 dB in the E-plane and to −40.5 dB from −25.4 dB in the H-plane. Figure 11(c) shows the radiation patterns of the cross polarization where ϕ are 0, 45 and 90 degrees.

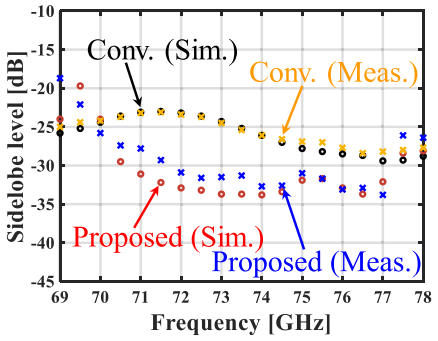

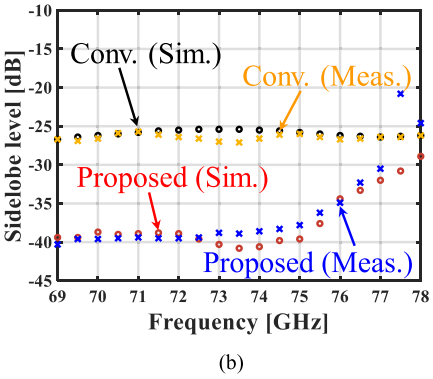

Fig. 12 Frequency characteristics of the sidelobe level at tilts around 30–40 degrees. (a) E-plane. (b) H-plane.

The level is normalized by the main polarization at the boresite. The maximum level of the cross polarization is −43 dB where ϕ is 45 degrees. The cross polarization at the boresite is suppressed due to the structural symmetry. The slit layer configuration does not affect the cross polarization. The effect to degrade the directivity of the main polarization by the cross polarization is negligible. Figure 12 shows the frequency characteristics of the sidelobe level at tilts around 30–40 degrees at 0.5 GHz intervals. The sidelobe level of the proposed antenna is suppressed over the desired range of frequencies among 71.0–76.0 GHz compared to the waveguide slot antenna without the slit layers (called as conventional antenna thereafter).

5. Measurement

A prototype of the proposed antenna is shown in Fig. 13 and photographs of the fabricated prototype are shown in Fig. 14. The conventional waveguide slot array antenna shown in the bottom of the panel of Fig. 13 is fabricated by diffusion bonding of laminated thin copper plates. The pattern of the layers is formed by etching a thin copper plate. The thickness of the copper plate is 0.2 mm, and the total thickness of the copper plates is 3.4 mm. The adding layers on the conventional antenna consist of the E-plane slit layer with the PTFE substrate, the H-plane slit layer, and the air layers 1 and 2 formed by the copper flames whose thickness is 0.2 mm and 0.3 mm, respectively, as shown at the top of Fig. 13. The

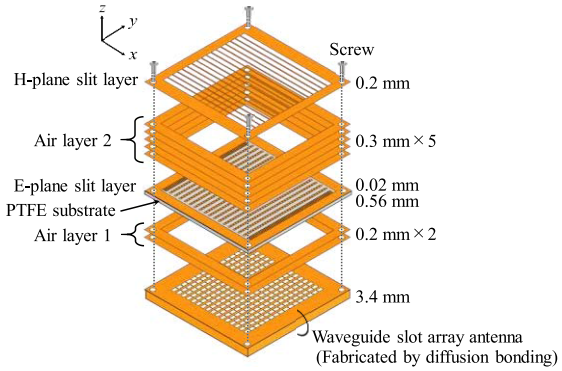

Fig. 13 The configuration of a prototype of the proposed antenna.

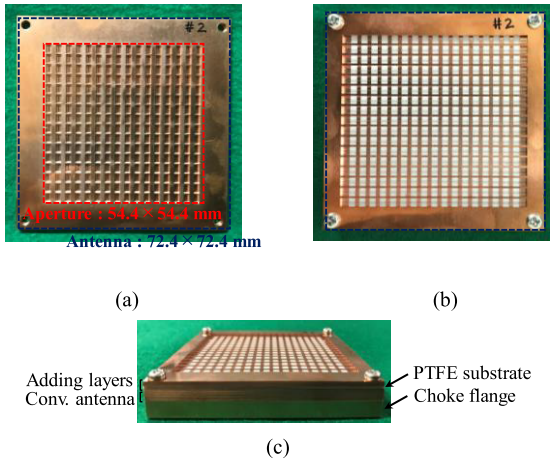

Fig. 14 Photographs of the fabricated prototype. (a) Top view of the conventional antenna. (b) Top view. (c) Side view.

E-plane slit layer is 0.018 mm thick and is formed by etching a 0.56 mm-thick copper-clad PTFE substrate, and the H-plane slit layer is 0.2 mm thick and is formed by etching. The adding layers are screwed onto the conventional antenna at the four corners. The size of the antenna is 72.4 mm × 72.4 mm × 6.1 mm. A choke flange with a 6.0 mm thickness is used to attach a standard rectangular waveguide WR-12 with the antenna by screws for the measurements.

Figure 15 shows the measured frequency characteristics of the reflection with the simulated values. The bandwidth for VSWR < 1.5 is 12.2% (69.9–78.9 GHz).

The measured frequency characteristics of the directivity and the realized gain are plotted in Fig. 10. The realized gain is measured by a W-band far-field measurement system for 69–78 GHz in an anechoic chamber. The measured directivity is estimated from the aperture field by near-field measurements. At the design frequency, the results are 32.9 dBi directivity, 77.6% aperture efficiency, 32.6 dBi realized gain, and 73.0% antenna efficiency. At the design frequency, the total conductor and PTFE losses are estimated to be 0.3 dB by the measured values of the reflection and the realized gain. The measured values of the directivity and the realized gain agree well with the simulated values.

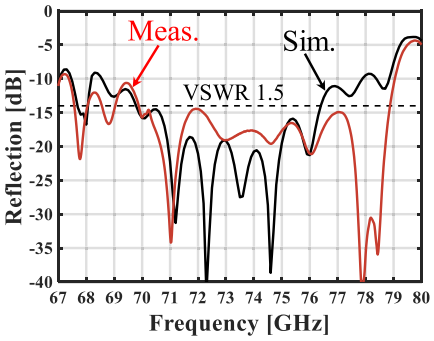

Fig. 15 Frequency characteristics of reflections in the measurements.

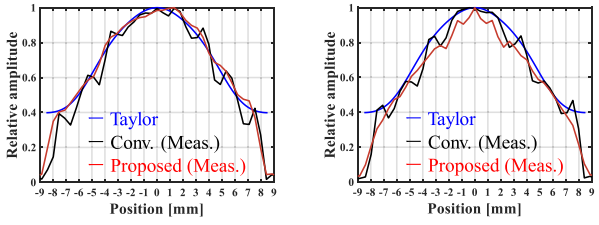

Fig. 16 Aperture field distributions at the design frequency. (a) E-plane. (b) H-plane.

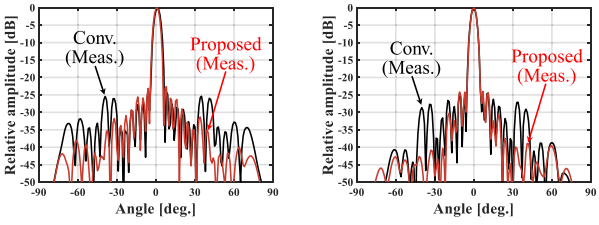

Fig. 17 Radiation patterns at the design frequency. (a) E-plane. (b) H-plane.

Figures 16 and 17 show the measured aperture field distributions and the radiation patterns at the design frequency. The aperture field in the proposed antenna agrees better with the Taylor distribution than that in the conventional antenna. In the radiation patterns in the proposed antenna, the sidelobe level at tilts around 30–40 degrees is suppressed below those in the conventional antenna, especially at the design frequency from −25.4 dB to −31.3 dB in the E-plane and from −27.1 dB to −38.9 dB in the H-plane. The measured frequency characteristic of the sidelobe level at tilts around 30–40 degrees with the simulated values at 0.5 GHz intervals is plotted in Fig. 12. The measured values are very similar to the simulated values, and the sidelobe level of the proposed antenna as shown as yellow marks is suppressed over the desired range of 71.0–76.0 GHz compared to the conventional antenna.

6. Conclusion

In this paper, we have reported the sidelobe suppression at tilts around 30–40 degrees in both the E and H planes due to the tapered excitation of units of 2×2 radiating slots by introducing slit layers over a corporate-feed waveguide slot array antenna. A 16×16-element array in the 70 GHz band incorporating this has been fabricated. At the design frequency, we have confirmed by the measurements the sidelobe levels at tilts around 30–40 degrees are suppressed from −25.4 dB to −31.3 dB in the E-plane and from −27.1 dB to −38.9 dB in the H-plane, and the sidelobe levels are suppressed over the desired range of 71.0–76.0 GHz frequencies, compared to the conventional antenna.

References

[1] Fixed Radio System Characteristics Requirements, Standard ETSI EN 302 217-4-2 V1.5.1 (2010-01), European Telecommunications Standards, 2010. [Online]. Available: http://www.etsi.org/index.php
[2] A. Vosoogh, P. Kildal, and V. Vassilev, "Wideband and high-gain corporate-fed gap waveguide slot array antenna with ETSI class II radiation pattern in V-band," IEEE Trans. Antennas Propag., vol.65, no.4, pp.1823–1831, Dec. 2016.
[3] L. Shi, C. Bencivenni, R. Maaskant, J. Wettergren, J. Pragt, and M. Ivashina, "High-efficiency and wideband aperiodic array of uniformly excited slotted waveguide antennas designed through compressive sensing," IEEE Trans. Antennas Propag., vol.67, no.5, pp.2992–2999, Jan. 2019.
[4] D. Shin, K. Kim, J. Kim, and S. Park, "Design of low side lobe level millimeter-wave microstrip array antenna for automotive radar," Proc. International Symposium on Antennas & Propag., Oct. 2013.
[5] D. Nakazawa, K. Sakakibara, N. Kikuma, and H. Hirayama, "Low-sidelobe design of microstrip comb-line antennas for beam-tilting in perpendicular plane to feeding line," Intl. Symp. Antennas Propag., Dec. 2014.
[6] E. Rahardjo, E. Sandi, and F. Zulkifli, "Design of linear sparse array based on the Taylor line source distribution element spacing," APMC, May 2018
[7] J. Cao, Y. Liu, Y. Wang, and R. Han, "Design of a new microstrip antenna array with high gain and low side-lobe," ICMMT, Dec. 2018.
[8] R. Shaw and M. Mandal, "Backfire microstrip leaky-wave antenna with reduced sidelobe and low cross polarization," IEEE Antennas Wireless Propag. Lett., vol.18, no.6, pp.1218–1222, April 2019.
[9] K. Kojima, T. Taniguchi, M. Nagayasu, Y. Toriyama, and M. Zhang, "A study of interference canceller for DDD system on millimeter-wave band fixed wireless access system," Euro. Conf. Antennas Propag., C10-10, April 2015.
[10] C.A. Balanis, Antenna Theory: Analysis and Design, 3rd ed., pp.406–408, John Wiley & Sons, 2005.
[11] M. Zhang, J. Hirokawa, and M. Ando, "Double-layer plate-laminated waveguide slot array antennas for a 39 GHz band fixed wireless access system," IEICE Trans. Commun., vol.E97-B, no.1, pp.122–128, Jan. 2014.
[12] M. Zhang, J. Hirokawa, and M. Ando, "A four-corner-fed double-layer waveguide slot array with low sidelobes developed for a 40 GHz-band DDD system," IEEE Trans. Antennas Propag., vol.64, no.5, pp.2005–2010, May 2016.
[13] Y. Miura, J. Hirokawa, M. Ando, Y. Shibuya, and G. Yoshida, "Double-layer full-corporate-feed hollow-waveguide slot array antenna in the 60-GHz band," IEEE Trans. Antennas Propag., vol.59, no.8, pp.2844–2851, Aug. 2011.
[14] Y. Watarai, M. Zhang, J. Hirokawa, and M. Ando, "Sidelobe suppression in a corporate-feed double-layer waveguide slot array antenna," Intl. Symp. Antennas Propag., FrD1-5, Oct. 2011.
[15] R.W. Haas, D. Brest, H. Mueggenburg, L. Lang, and D. Heimlich, "Fabrication and performance of MMW and SMMW platelet horn arrays," Intl. J. Infrared Milli. Waves, vol.14, no.11, pp.2289–2294, Jan. 1993.
[16] G.L. Huang, S.G. Zhou, T.H. Chio, H.T. Hui, and T.S. Yeo, "A low profile and low sidelobe wideband slot antenna array fed by an amplitude-tapering waveguide feed-network," IEEE Trans. Antennas Propag., vol.63, no.1, pp.419–423, Jan. 2015.
[17] L. Chin, Y. Lu, Q. You, Y. Wang, J. Huang, and P. Gardner, "Millimeter-wave slotted waveguide array with unequal beamwidths and low sidelobe levels for vehicle radars and communications," IEEE Trans. Antennas Propag., vol.67, no.11, pp.10574–10582, Nov. 2018.
[18] H. Arakawa, H. Irie, T. Tomura, and J. Hirokawa, "Suppression of E-plane sidelobes using a double slit layer in a corporate-feed waveguide slot array antenna consisting of 2×2-element radiating units," IEEE Trans. Antennas Propag., vol.67, no.6, pp.3743–3751, June 2019.

Haruka Arakawa was born in Tokyo, Japan. She received the B.S. and M.S. degrees in electrical and electronic engineering from the Tokyo Institute of Technology, Tokyo, Japan, in 2017 and 2019, respectively. She currently works at Murata Manufacturing Corporation, Kyoto.

Takashi Tomura was born in Sendai, Japan. He received the B.S., M.S. and D.E. degrees in electrical and electronic engineering from the Tokyo Institute of Technology, Tokyo, Japan, in 2008, 2011 and 2014, respectively. He was a Research Fellow of the Japan Society for the Promotion of Science (JSPS) in 2013. From 2014 to 2017, he worked at Mitsubishi Electric Corporation, Tokyo and was engaged in research and development of aperture antennas for satellite communications and radar systems. He is currently a Specially Appointed Assistant Professor at the Tokyo Institute of Technology, Tokyo. His research interests include electromagnetic analysis, aperture antennas and planar waveguide slot array antennas. Dr. Tomura received the Best Student Award from Ericsson Japan in 2012 and the IEEE AP-S Tokyo Chapter Young Engineer Award in 2015. He is a member of IEEE and IEICE.

Jiro Hirokawa received the B.S., M.S. and D.E. degrees in electrical and electronic engineering from Tokyo Institute of Technology (Tokyo Tech), Tokyo, Japan in 1988, 1990 and 1994, respectively. He was a Research Associate from 1990 to 1996 and an Associate Professor from 1996 to 2015 at Tokyo Tech. He is currently a Professor there. He was with the antenna group of Chalmers University of Technology, Gothenburg, Sweden, as a Postdoctoral Fellow from 1994 to 1995. His research area has been in slotted waveguide array antennas and millimeter-wave antennas. He received IEEE AP-S Tokyo Chapter Young Engineer Award in 1991, Young Engineer Award from IEICE in 1996, Tokyo Tech Award for Challenging Research in 2003, Young Scientists' Prize from the Minister of Education, Cultures, Sports, Science and Technology in Japan in 2005, Best Paper Award in 2007 and a Best Letter Award in 2009 from IEICE Communications Society, and IEICE Best Paper Award in 2016 and 2018. He is a Fellow of IEEE and IEICE.